Published by :
https://www.ijert.org/
An International Peer-Reviewed Journal

International Journal of Engineering Research & Technology (IJERT)
ISSN: 2278-0181
Vol. 15 Issue 11 , November - 2026

A Soft Computing Approach for Estimating In situ Compressive Strength of PCE based Pervious Concrete Using UPV and Rebound Hammer Test

Dr. Bharti Tekwani
Structural Engineering Department, Ph.D.
MBM University, Jodhpur, Rajasthan,
342011 India,

Dr. Archana Bohra Gupta
Structural Engineering Department, Professor,
MBM University, Jodhpur, Rajasthan, 342011
India,

***Abstract* - Pervious concrete pavement effectively meets environmental demands by allowing surface water to percolate through its voids. Its key distinguishing features from conventional concrete include the type and gradation of coarse aggregates, the proportion of no fines or little fines and cement type used in the mix. This study focuses on developing a mathematical model using artificial neural networks (ANN) incorporating NDT to predict the in situ compressive strength of pervious concrete manufactured as a conglomerate of cement, coarse aggregate and Poly carboxylate ether (PCE) based admixture. Data obtained from experimental work, encompassing both NDT results as input and destructive testing results as output variables, is utilized to train the ANN network. From the results of the ANN model (specifically the weights and biases) mathematical equations are derived using leaky ReLU activation functions for determining compressive strength of pervious concrete up to 30 MPa from NDT values.**

Keywords* - *ANN, PCE Pervious concrete, Rebound hammer, Regression Equations, ultrasonic pulse velocity

I. INTRODUCTION

Pervious concrete (P_C) is a distinctive type of permeable concrete characterized by its enhanced porosity and high permeability due to its large pore size and continuous void structure, which typically contains 15 to 35% void content. To ensure proper performance, a minimum void content of 15% is essential, particularly formed as no fine concrete [1]. Research by Meininger (1988) [2] indicates that an optimal water-cement ratio (w/c) of 0.35 to 0.45 is critical to avoid bowling in mixture and to ensure effective coating of aggregate with cement paste. The strength of pervious concrete (φ) and permeability (ρ) typically exhibit inverse relationship for P_C. Increasing the percentage of fines can enhance φ, but often leads to decrease of ρ. To optimize both φ and ρ, reducing fine aggregate content and using suitable admixture can be an effective strategy.

Research on determining ρ and optimal w/c for P_C was initiated by Meininger (1988) [2]. The Falling head method and Tomography techniques were employed to measure ρ and analyse the pore network for P_C respectively [3]. Further studies calculate ρ values alongside the φ for various concrete using 9.375 mm and 18.75 mm aggregates across three different cement aggregate ratios (C/A). The finding indicates that smaller aggregate size can effectively balance both φ and ρ, leading to recommendation of using Constant Head Permeameter for accurate ρ determination [4, 5]. Additionally, a control mix demonstrate the potential to achieve maximum φ up to 30 MPa while maintaining ρ values between 57.8 and 299.5 inch per hour at a restricted water cement ratio of 0.35 [6]. Addition of polycarboxylate ether (PCE) admixture replacing 0.35% of cement mass improved workability, reducing water demand by 18% and with a w/c ratio of 0.23 achieved optimal φ above 20 MPa [26].

The φ of P_C can be enhanced by adding admixtures such as pozzolan, including silica fume and ground granulated blast furnace slag (GGBS). In GGBS based P_C for a given porosity (σ), the use of recycled concrete aggregate (RCA) resulted in a reduction in the φ of P_C. However, the influence of aggregate type on φ diminished nonlinearly as σ increased. Strength correlation of using natural and RCA respectively are $\varphi_N = 70.2e^{-0.066\sigma}$; $\varphi_{RCA} = 22.2e^{-0.052\sigma}$ .Furthermore, the ρ of P_C was primarily governed by its σ, as shown by $\rho = 1.93e^{0.0755\sigma}$ and the incorporation of RCA had no significant impact on its ρ. [25]. In GGBS based P_C, φ decreased from 22.4 MPa (control mix) to 20.2 MPa and 15.6 MPa when 20% and 40% RCA were used, respectively. Similarly, replacing fine aggregate with recycled fine glass (RFG) at 50% and 100% resulted in reductions in φ by approximately 2% and 17% respectively. When both RCA (20–40%) and RFG (50–100%) were incorporated simultaneously, the φ of the P_C ranged from 17.5 MPa to 11.9 MPa, representing a 22–47% reduction compared to the control mixture [27]. Silica fume is a by-product of silicon production contained high percentage of silicic acid and feature tiny particles with large surface area. This makes it effective supplementary cementitious material that increases the density and strength of concrete. The high content of silicic acid up to 90% enhances the property of calcium silicate hydrate (CSH) gel, promoting better bonding between cement binder and aggregate [7]. L.Wu et al. investigated the performance of photocatalytic pervious concrete (TPC) containing varying amounts of nano particle TiO_2 (0–8%) for purifying methyl orange (MO) from polluted water. Results show that the photocatalytic efficiency increases with TiO_2 content up to 5%, achieving a maximum degradation rate of 42.8% at 120 minutes, but declines beyond this point. However, higher TiO_2 content reduces compressive strength significantly from 26.0 MPa to 13.5 MPa as it impairs cement hydration. Among all mixes, 2% TiO_2 was found optimal, balancing mechanical strength, porosity, photocatalytic efficiency, and TiO_2 utilization. Compared to ordinary concrete, TPC exhibited superior adsorption, degradation, and utilization rates, highlighting its potential in sustainable urban pollution control [28].

(This work is licensed under a Creative Commons Attribution 4.0 International License.)

International Journal of Engineering Research & Technology (IJERT)
ISSN: 2278-0181
Vol. 15 Issue 11 , November - 2026

In another study, P_C mixes incorporating 20% fines, w/c of 0.30 and aggregate size of 5mm to 10 mm and 15mm to 25mm were tested. The result demonstrated that the inclusion of 20% fine enhance UPV, flexure strength and φ while only slightly reducing ρ (Yazici and Aghabaglou, 2017) [8]. SVM model had been developed to predict ρ coefficient and unconfined φ for influencing parameters selected as varying cement-aggregate ratio (C/A), w/c and aggregate size the model yields highest accuracy in terms of coefficient of determination (R^2) 0.98 for ρ coefficient and 0.99 for unconfined φ model [9].

NDT methods are essential for evaluating material property without significantly damage the structure. The Schmidt rebound hammer (R_{SN}) [10] and ultrasonic pulse velocity (μ) [11] can be employed to estimate φ of P_C through appropriate mathematical models. Both R_{SN} and μ are indicators of concrete quality, but they do not directly measure φ. Therefore, a correlation between R_{SN}, μ and φ is necessary for evaluating in situ φ. Polynomial regression or basic curve fitting statistical regression approach provides a straight forward approach to construct regression equations for correlation of NDT results and φ [12], while ANN offers a more advanced heuristic model for correlating input –output data and achieving effective results. ANNs composed of artificial neuron and are designed to learn from data, recognize patterns, classify data and predict outcomes. They are simply suitable for supervised learning and non -linear relationships [19]. The predicted outcome depends upon the number of neurons in neural network which are selected by trial and error process and suitable activation functions are applied on each layer [13].

For pervious concrete μ values were observed less than 2 km/ sec at 28 days of testing. This limit indicates samples as weak concrete [14]. For estimated φ ranges 2.14 MPa to 28.35 MPa of samples, μ values vary between 2.28 km/s and 4.42 km/sec with the average value 3.44 km/sec. Power correlation eqaution had been derived as $\varphi = 0.1292\ \mu^{3.617}$ [15].

Tekwani and Gupta (2024) [16] investigated strength of pervious concrete samples incorporating silica fume and ground granulated blast furnace slag (GGBS) replacing 10–11% of cement, which matched average M20 grade concrete in both cases with use of naphthalene based admixture. NDT, specifically determining R_{SN} and μ were performed on the samples. After collecting sufficient NDT readings, destructive testing (DT) was carried out to determine the actual compressive strength. Correlation equations (Table 1) were developed using both curve fitting techniques and artificial neural network (ANN) algorithms with Tan sigmoid activation functions in both hidden layer and output layer. With the incorporation of these supplementary cementitious materials (SCMs), the compressive strength of the samples was observed to reach up to 20 MPa while also slightly reducing ρ.

Table 1 General Equations for predicting φ of Pervious concrete with Silica fume and GGBS using Cftool and ANN (Tekwani and Gupta 2024)

Tool	Regression Equation
Cftool	$\varphi = 1.289 + 1.013\ R_{SN} + 0.01809\ \mu$
ANN	$A_1 = -4.4272 + 0.047984R_{SN} + 3.209091$
	$A_2 = 3.379 - 0.31161R_{SN} - 2.74858\mu$
	$A_3 = 2.7345 - 0.54677R_{SN} - 0.87651\mu$
	$A_4 = 2.377 - 0.5428R_{SN} + 0.869309\mu$
	$A_5 = -0.24746 + 0.64292R_{SN} + 1.083345$
	$A_6 = 0.96182 + 0.292787R_{SN} - 2.75782\ \mu$
	$A_7 = -0.73613 - 0.47953R_{SN} + 1.019782$
	$A_8 = 2.5637 + 0.382387R_{SN} - 2.43156\ \mu$
	$A_9 = 3.905 + 0.6054R_{SN} + 1.209964\ \mu$
	$A_{10} = 3.9308 + 0.34096R_{SN} + 2.206036\mu$
	$B_1 = 0.080777\,\mathrm{TANH}(A_1)$
	$B_2 = 0.27369\,\mathrm{TANH}(A_2)$
	$B_3 = -0.22511\,\mathrm{TANH}(A_3)$
	$B_4 = 1.9756\,\mathrm{TANII}(A_4)$
	$B_5 = 1.5731\,\mathrm{TANH}(A_5)$
	$B_6 = 0.17887\,\mathrm{TANH}(A_6)$
	$B_7 = -1.0732\,\mathrm{TANII}(A_7)$
	$B_8 = -0.4479\,\mathrm{TANH}(A_8)$
	$B_9 = -0.87483\,\mathrm{TANH}(A_9)$
	$B_{10} = 0.91889\,\mathrm{TANH}(A_{10})$
	$b_{0=}$ -0.059395
	$\varphi_n = \mathrm{TANH}\ b_0 + \sum_{i=1}^{10} B_i$
	$\varphi = 8.5 \times \varphi_n + 13.5$

The equations derived using the Curve Fitting Tool (cftool) and Artificial Neural Network (ANN), as presented in Table 1, correspond to a rebound number range of 7–22 and a pulse velocity (μ) range of 2.0–4.7 km/sec and is suitable for pervious concrete strength upto 20 MPa. This is the minimum range of concrete design mix strength and has limited applications. Hence, further research was needed to find ways to enhance the φ of P_C for wider usage.

The present study, conducted as part of a research series aimed at enhancing the φ of P_C by utilizing a PCE admixture in place of naphtalene based admixture and dropping the use of SCMs. PCE superplasticizers are ideal for OPC 53-grade cement because they enhance workability, strength, and durability while supporting sustainable, low-water concrete mix designs [17].

2. TESTING

2.1 Design Mix and Testing Procedure

Experimental study- 150 cubes of P_C with a cross section area of 150mm × 150 mm were cast in the laboratory of at MBM University, Jodhpur, India. The raw material used in the study is detailed below.

(This work is licensed under a Creative Commons Attribution 4.0 International License.)

International Journal of Engineering Research & Technology (IJERT)
ISSN: 2278-0181
Vol. 15 Issue 11 , November - 2026

- Cement- Ordinary Portland cement of Ultratech cement brand of 53 grade; [22]
- Coarse Aggregate- Rounded crushed aggregate of size 10mm from Kakani quarry, Jodhpur Rajasthan;
- Fine Aggregate- Sand (Zone II) locally sourced;
- Water- Portable water is used for casting and curing of all specimens;
- Admixture- PCE based admixture (SP), dosage 0.35% of cement weight.

Mix design was carried out using specifications in accordance with the guidelines of ACI 522R, 2010 [18] provided in Table 2.

Table 2 Design Mix Parameters per m^3 Pervious Concrete

Cement kg	CA (10mm) kg	C/A	SP Kg	w/c
440	1320	1:3	1.54	0.45

These materials were dry mixed for approximately 2-3 minutes to ensure uniform distribution. After dry mixing, 20% of the total water was introduced to the mix, resulting in a pre-wet mix. The mixture was blended further to ensure even hydration. The super plasticizer, along with the remaining water as per Table 2 was then added to mix. Mixing continues for an additional 8-10 minutes until a uniform color and consistency were achieved. The mix is considered ready when it exhibits the desired consistency, which was determined by the "ball test". To perform this test, a tightly compressed ball of concrete was formed by hand and held for 5-10 seconds. Upon release, the ball should break when dropped back into mix. It did. This indicated that the mix had the correct water content. After mixing the P_C is transferred to collected tray and then placed into a properly oiled mould. The mix is compacted in three layers with each layer receiving 35 strokes using a tamping rod, following the guideline outlined in IS 1199 (Part 5) - 2018 [22].

2.2 Permeability Test

The permeability test of Pervious Concrete was evaluated by using the methodology referred to in ASTM C 1701/C [29]. In this test, both side open cylinder is used for field tests with standard specifications. Since, as per Indian Standard specifications, cubes are used for testing, a both side open cubical container with similar specifications as in the above mentioned standard was used for measuring the permeability.

Table 3 Observations for permeability test

Length (mm)	Diameter (mm)	Water head (mm)	Time (s)	Average ρ(mm/s)
200	100	200	2.94	68.03

2.3 NDT Data Acquisition

Data collection had been done using NDT (R_{SN}, μ) and DT (φ using compression testing machine (CTM)) in MBM University laboratory. Assembling of data for each concrete type was carried out using both DT and NDT respectively. Compressive strength in MPa of the cubes was determined using DT (compressive strength test) as per IS 516: 2021 [21]. Meanwhile, NDT (R_{SN} and μ tests) were carried out as per IS 516: Part 5 /Sec 4 – 2020 [11] and IS: 516 Part 5 /Sec 1- 2018 [10] respectively. In this study, Schmidt rebound hammer N type with 2.207 N-m impact energy was used. The value of φ test and R_{SN} test were taken simultaneously on concrete cubes. R_{SN} readings in vertical direction were taken on surfaces. Nine readings were taken on each of two vertical opposite faces.

Direct transmission (cross probing) refers to the direction of wave propagation. To measure the transit time accurately, a good contact needs to be ensured between the transducers and the concrete surface. Three transit time measurements were taken on each pair of opposite sides, resulting in a total of six measurements by cross probing. The μ test in this direction was determined using the mean value of these six measurements.

The data obtained from testing was subjected to simple statistical analysis to enable it to be used for ANN training and testing. The results are summarized in Table 4.

Table 4 Descriptive Range of Data for ANN Training and Testing

Var.	Mean	Median	Mode	SD	Range	Min	Max	Count
R_{SN}	15.05	15	15	2.67	11	8	19	150
μ(km/sec)	4.16	3.98	3.15	0.89	3.4	3	6.4	150
Φ (MPa)	26.49	27	28	2.50	9.5	21	30.5	150

3. MODEL

3.1 Polynomial Regression Method (Curve Fitting)

Polynomial equations were developed using linear regression using "cftool" in MATLAB. Fitness was evaluated by viewing goodness of fit statistics, confidence intervals (95%) and residuals.

Equation 1 is general form of equation in "*cftool*".

$$f(x,y) = P_0 + P_{10} \times x + P_{01} \times y \qquad (1)$$

Where, P_0, P_{10} *and* P_{01} are the coefficients with 95% confidence level [12].

Regression Equation developed using Statistical Regression (cftool) is given by equation (2)

$$\varphi = 25.51 + 0.033R_{SN} + 0.168\mu, R^2 = 0.631 \quad (2)$$

3.2 ANN Model

(This work is licensed under a Creative Commons Attribution 4.0 International License.)

International Journal of Engineering Research & Technology (IJERT)
ISSN: 2278-0181
Vol. 15 Issue 11 , November - 2026

Inspired by biological neuron, ANN consists of multiple processing layers with simple operational elements. A typical network includes an input layer and one or more hidden layers. Each layer comprises interconnected neurons or nodes, with the output of one layer serving as input for the next [13, 19].

In this study leaky ReLU activation function was used. The Hyperbolic tangent function (TANH) is commonly used in shallow neural network which process sequential data. TANH helps the network learn by reflecting the current output based on previously trained input. However, these types of network often face challenges related to gradient size, specifically issue of exploding or vanishing gradients. To mitigate these issues, researcher often recommended using the number of hidden layer. On other hand, the Rectified Linear Unit (ReLU) is typically employed in multilayer perceptron. ReLU addresses the venous ingredient problem effectively, as its derivative is either 0 or 1. When the input is positive, the derivative equals one, while it becomes zero for negative inputs, leading to phenomenon known as "dying ReLU". This means that neuron can become inactive and fail to learn. To overcome the dying ReLU issue, the parametric Rectified Linear Unit (PReLU) has been introduced, defined by the equation $f(x) = max(\alpha x, x)$. In this formulation, Alpha is set to 0.01 the parametric value function becomes leaky ReLU, allowing a small nonzero gradient for negative inputs. This enhances the model ability to learn and maintain active neuron throughout training [23]. Table 5 shows the parameters used in ANN modeling.

Table 5 Parameter used for ANN modelling

Parameters	Description
Records	150
Number of layer	3
Training	70%
Testing	15%
Validation	15%
Number of neurons	10
Training algorithm	trainlm ('Levenberg-Marquardt Backpropagation').
Epochs	5
Error	MSE

The input data has been employed in order to predict the target values using ANN tool (nftool) in MATLAB© version R2017b. The optimal dataset for training encompasses the full modeling domain with minimal repetitive samples. Therefore, 70% of data is used for training, 15% for validation and 15% remaining is reserved for testing. The network is trained using back propagation (BP) technique with the input data spanning between minimum to maximum values. The BP network structure consists of the three layers: an input layer, a hidden layer, and an output layer enabling data flow from input to output and vice versa. In this study, R_{SN} and μ serve as the independent input variables, while the φ is the dependent variable.

The selection of number of neurons in the hidden layer follows a trial and error approach. Initially a trial number of neurons is chosen, then after analysis, if error value is high, the number of neurons is changed. Thus, the network architecture included two neurons in input layer, one neuron in the output layer and 10 neurons in the hidden layer, for achieving optimum performance. The Levenberg-Marquardt Backpropagation algorithm (trainlm) is used for the training the network. Fig.1 showed the regression plots and MSE error at epoch 5.

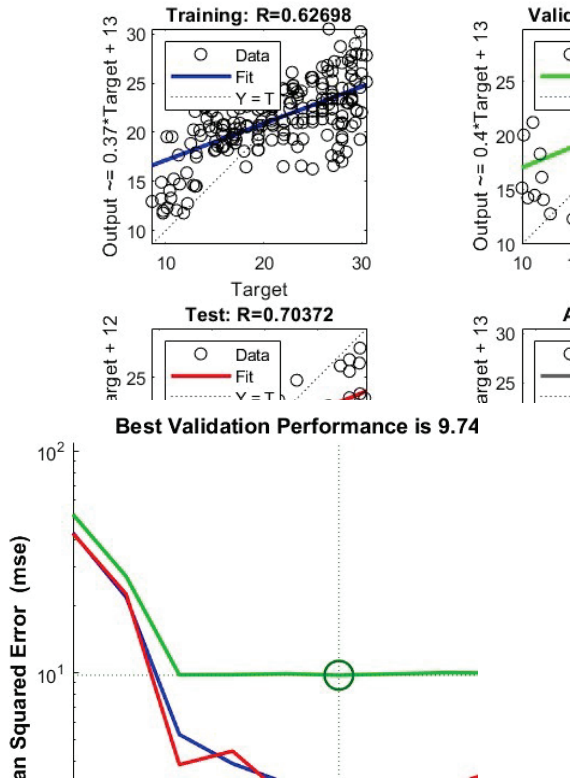


Fig. 1 Regression Plots and MSE performance of Proposed ANN Model

An algorithm was developed to derive mathematical equations from trained data using Tanh activation function alongside ANN mathematical model by using Eq. 3.

$$y = f_a\left[T_0 + \sum_{k-1}^{k=h}\left\{w_k \times f_a\left(T_{hk} + \sum_{i-1}^{i=m} w_{ik}x_i\right)\right\}\right] \quad (3)$$

where y is normalized or unstructured variable (φ), f_a is Tanh activation function, $x_i (= R_{SN}, \mu)$ is normalized input of variable i; $w_{ik}$is connected weight of i^{th} input variable to hidden layer; h=10 is number of neurons in the hidden layer; T_{hk} is bias at k^{th} neuron of hidden layer; $w_k$is connected weight between k^{th} neuron of hidden layer and single output; T_0 is bias at output layer.

(This work is licensed under a Creative Commons Attribution 4.0 International License.)

International Journal of Engineering Research & Technology (IJERT)
ISSN: 2278-0181
Vol. 15 Issue 11 , November - 2026

$$P_k = T_{hk} + \sum_{i=1}^{i=m} (w_{ik} R_{SN} + w_{ik}\mu) \qquad (1)$$

$$Q_k = w_k \times T\,max(P_K, 0.01P_K) \qquad (5)$$

$$R = T_0 + \sum_{k=1}^{k=h} Q_k \qquad (6)$$

$$\varphi_n = max(R, 0.01R) \qquad (7)$$

The input and output parameters were normalized within the range of −1 to +1 to ensure dimensional consistency and numerical stability. Equation 2.3 used to scale the input parameters. This scaling is compatible with the adopted for TANH and Leaky ReLU activation functions, which allows a small non-zero gradient for negative inputs, thereby preventing neuron inactivation and improving learning efficiency.

$$M_i = \frac{(M_{max} - M_{min})(N_i - N_{min})}{(N_{max} - N_{min})} + M_{min} \qquad (2.3)$$

Where M_i is the normalized (scaled) value, M_{max} and M_{min} represent the upper and lower limits of the scaling range (−1 and +1, respectively), N_i is the original value of the parameter, and N_{max} and N_{min} denote the maximum and minimum values of the original dataset.

The normalized variable P_1 to P_{10} , Q_1 to Q_{10} in Eq. 5 are unknown and can be computed using Eq. 3 using data from Table 4. The weights and biases for the hidden neurons, obtained from ANN analysis are represented in Table 6. The equations for determining P, Q, T_0, R, φ_n and φ are expressed in Table 7.

Table 6 Weights and Bias obtained from ANN Simulation

Hidden neurons	Weights R_{SN}	Weights μ	Weights φ	Biases b_{hk}	Biases b_0
K_1	-3.8165	1.6016	-0.4274	4.4133	
K_2	1.5459	-3.5712	1.2489	-4.0128	
K_3	1.4047	3.9194	0.4973	-3.0218	
K_4	5.0215	-1.4952	-0.3593	-2.0062	
K_5	-1.3424	-4.2824	-0.2820	0.9698	0.7118
K_6	-2.5489	2.9300	-0.5145	0.8934	
K_7	-3.9940	-2.6531	-0.2086	-2.7736	
K_8	2.4109	-4.7698	0.7951	3.439	
K_9	-3.9082	-2.6449	-2.1948	-3.1409	
K_{10}	-6.0143	-0.0339	1.6907	-4.0741	

Table 7 General Equations for predicting φ using ANN

$$A_1 = 4.4133 - 3.8165R_S + 1.6016\mu$$
$$A_2 = -4.0128 + 1.5459R_S - 3.5712\mu$$
$$A_3 = -3.0218 + 1.4047R_S + 3.9194\mu$$
$$A_4 = -2.0062 + 5.0215R_S - 1.4952\mu$$
$$A_5 = 0.9698 - 1.3424R_S - 4.2824\mu$$
$$A_6 = 0.8934 - 2.5489R_S + 2.9300\mu$$
$$A_7 = -2.7736 - 3.9940R_S - 2.6531\mu$$
$$A_8 = 3.439 + 2.4109R_S - 4.7698\mu$$
$$A_9 = -3.1409 - 3.9082R_S - 2.6449\mu$$
$$A_{10} = -4.0741 - 6.0143R_S - 0.0339\mu$$

$$B_1 = -0.4274\ \max(A_1, 0.01A_1)$$
$$B_2 = 1.2486\ \max(A_2, 0.01A_2)$$
$$B_3 = 0.4973\ \max(A_3, 0.01A_3)$$
$$B_4 = -0.3593\ \max(A_4, 0.01A_4)$$
$$B_5 = -0.2820\ \max(A_5, 0.01A_5)$$
$$B_6 = -0.5145\ \max(A_6, 0.01A_6)$$
$$B_7 = -0.2086\ \max(A_7, 0.01A_7)$$
$$B_8 = 0.7951\ \max(A_8, 0.01A_8)$$
$$B_9 = -2.1948\ \max(A_9, 0.01A_9)$$
$$B_{10} = 1.6907\ \max(A_{10}, 0.01A_{10})$$

$$b_{0=}0.7118$$

$$C = b_0 + \sum_{i=1}^{10} B_i$$

$$f_n = \text{TANH}\ C$$

$$f_{PC3}=4.75\times(f_{nPC3} + 1) + 21$$

4. RESULTS AND DISCUSSION

Various empirical equations have been used to predict the φ of conventional concrete using R_{SN} and μ tests. However, these correlation equations have proven inaccurate for P_C. This study proposes an ANN based non linear approach and statistical linear model (cftool) to predict φ using NDT and DT results obtained from laboratory experiments on P_C cubes. This study focused on developing P_C without fine aggregates and with the use of PCE admixture. Addition of this admixture enhanced the strength of P_C, giving values up to 30 MPa. The φ obtained from *ANN* model represented by Eq. (8) is compared with actual measured values obtained in laboratory. The Error Matrices for predictive and actual values of **φ** are represented by Table 8.

Table 8 Performance of predictive and actual values

Errors	Models		
	cftool	ANN (predicted)	ANN (actual)
$RMSE = \sqrt{\frac{1}{N}\sum_{i=1}^{n}(P_t - M_t)^2}$	2.42	1.90	1.92

(This work is licensed under a Creative Commons Attribution 4.0 International License.)

International Journal of Engineering Research & Technology (IJERT)
ISSN: 2278-0181
Vol. 15 Issue 11 , November - 2026

$MAPE = \frac{1}{N}\left[\sum_{i=1}^{n}\left\{\frac{\lvert M_i - P_i\rvert}{M_i}\right\} \times 100\right]$	9.52	7.45	8.4
$VAF = \left[1 - \frac{var(M_i - P_i)}{varM_i}\right] \times 100$	95	93.11	95.2

Where P is predicted, M is measured values and N is number of samples used for validation.

5. CONCLUSION

Using PCE admixture the strength of P_C sample had been increases up to 30 MPa.

The R_{SN} test reading are not much affected sometimes no reading had observed but μ readings are significantly changes due to porosity in pervious samples.

The linear correlation is proposed by equation 2 concluded φ of P_C for given dataset with RMSE value 2.42.

The performance of the proposed models both curve fitting and ANN were evaluated using statistical metrics such as mean absolute percentage error (MAPE), root mean square error (RMSE), and variance (VAF) shown in Table 8.

The proposed iteration equations shown in Table 6 are derived from the ANN model using the Leaky ReLU activation function in the hidden layer, which provides a better fit due to its non-linearity and demonstrates strong performance in predicting the φ of pervious concrete within the range of the database.

REFERENCES

[1] Malhotra, V.M. (1976). No-Fines Concrete—Its Properties and Application. ACI Journal Proceedings, 73(11), 628–644.

[2] Meininager, R.C. (1988). No Fines Pervious Concrete for Paving. Concrete International, 10(Aug), 20–27.

[3] Neithalath, N. (2004). Development and Characterization of Acoustically Efficient Cementitious Materials. PhD Thesis, Purdue University, West Lafayette, IN, 269 pp.

[4] Ajamu, S.O., Jimah, A.A., & Oluremi, J.R. (2012). Evaluation of Structural Performance of Pervious Concrete in Construction. International Journal of Engineering and Technology, 2(5).

[5] Crounch, L.K., Smith, N., Walker, A.C., Dunn, T.R., & Sparkman, A. (2006). Determining Pervious PCC Permeability with a Simple Triaxial Flexible-Wall Constant Head Permeameter. TRB 85th Annual Meeting Compendium of Papers, 18 pp.

[6] Ayyappan, A., Dinesh Kumar, D., Sangeetha, G., Roshini, S., & Sivasangari, M. (2018). Experimental Study on Pervious Concrete. International Journal of Scientific Development and Research (IJSDR).

[7] Liu, H., Luo, G., Wang, L., Wang, W., Li, W., & Gong, Y. (2019). Laboratory Evaluation of Eco-Friendly Pervious Concrete Pavement Material Containing Silica Fume. Applied Sciences.

[8] Yazici, S., & Aghabaglou, A.M. (2016). Effect of Aggregate Grain Size Distribution on Properties of Permeable Concrete. Journal of Fundamental and Applied Sciences, 9, 323–338.

[9] Sun, J., Zhang, J., Gu, Y., Huang, Y., Sun, Y., & Ma, G. (2019). Prediction of Permeability and Unconfined Compressive Strength of Pervious Concrete Using Evolved Support Vector Regression. Construction and Building Materials, 207, 440–449. https://doi.org/10.1016/j.conbuildmat.2019.02.117

[10] Bureau of Indian Standards (2018). IS 516 (Part 5/Sec 1): Non-Destructive Testing of Concrete—Ultrasonic Pulse Velocity Test, New Delhi, India.

[11] Bureau of Indian Standards (2020). IS 516 (Part 5/Sec 4): Non-Destructive Testing of Concrete—Rebound Hammer Test, New Delhi, India.

[12] Smalheiser, N.R. (2017). Correlation and Other Concepts You Should Know (Chapter 13). In Data Literacy: How to Make Your Experiments Robust and Reproducible (pp. 169–185). Academic Press. https://doi.org/10.1016/B978-0-12-811306-6.00013-0

[13] Tripathy, S., & Rath, D. (2018). Artificial Neural Network Prediction of Pervious Concrete Permeability and Compressive Strength. International Journal of Engineering Management, Humanities and Social Science Paradigms, 30, ISSN: 2347-601X.

[14] Whitehurst, E.A. (1951). Soniscope Test Concrete Structure. Journal of the American Concrete Institute, 47, 443–444.

[15] Sathiparan, N., Jeyananthan, P., & Subramaniam, D.N. (2024). Surface Response Regression and Machine Learning Techniques to Predict the Characteristics of Pervious Concrete Using Non-Destructive Measurement: Ultrasonic Pulse Velocity and Electrical Resistivity. Measurement, 229, 113241. https://doi.org/10.1016/j.measurement.2023.113241

[16] Tekwani, B., & Gupta, A.B. (2024). Predicting Compressive Strength of Pervious Concrete Using Artificial Neural Network and Regression. IOP Conference Series: Earth and Environmental Science, 1326(1), 012150.

[17] Lei, L., Hirata, T., & Plank, J. (2022). 40 Years of PCE Superplasticizers—History, Current State-of-the-Art and an Outlook. Cement and Concrete Research, 157, 106826. https://doi.org/10.1016/j.cemconres.2022.106826

[18] American Concrete Institute (2010). ACI 522R-10 Report on Pervious Concrete, Chapter 6: Pervious Concrete Mixing Proportioning, Farmington Hills, MI, USA.

[19] Ng, A. (2023). Machine Learning Notes. Stanford University. Available at: https://stanford.edu/materials/aimlcs229/cs229-notes1.pdf

[20] Bureau of Indian Standards (2015). IS 269:2015 – Ordinary Portland Cement – Specification (Sixth Revision), New Delhi, India.

[21] Bureau of Indian Standards (2021). IS 516:2021, Part 1—Testing of Strength of Hardened Concrete—Section 1: Compressive, Flexural and Split Tensile Strength, New Delhi, India.

[22] Bureau of Indian Standards (2018). IS 1199 (Part 5): Fresh Concrete—Method of Sampling, Testing and Analysis—Making and Curing of Test Specimens, New Delhi, India.

[23] Annamalai, V., & Prakash, N. (2021). Leaky ReLU Based Deep Neural Network for Classification of Brain Tumor in MRI Images. Traitement du Signal, 38(3), 825–831. https://doi.org/10.18280/ts.380331

[24] Ogunleye, A., & Wang, Q.-G. (2023). Deep Neural Network Model for Prediction of Concrete Compressive Strength Based on Leaky ReLU and Adam Optimizer. Engineering Applications of Artificial Intelligence, 119, 105816. https://doi.org/10.1016/j.engappai.2022.105816

[25] Sriravindrarajah, R., Wang, N.D.H., & Ervin, L.J.W. (2012). Mix Design for Pervious Recycled Aggregate Concrete. International Journal of Concrete Structures and Materials, 6(4), 239–246. https://doi.org/10.1007/s40069-012-0024-x

[26] Cai, J., Chen, J., Shi, J., Tian, Q., Xu, G., & Du, Y. (2022). A Novel Approach to Evaluate the Clogging Resistance of Pervious Concrete. Case Studies in Construction Materials, 16, e00864. https://doi.org/10.1016/j.cscm.2022.e00864

[27] El-Hassan, H., Kianmehr, P., Tavakoli, D., El-Mir, A., & Dehkordi, R.S. (2023). Synergic Effect of Recycled Aggregates, Waste Glass, and Slag on the Properties of Pervious Concrete. Developments in the Built Environment, 15, 100189. https://doi.org/10.1016/j.dibe.2023.100189

[28] Wu, L., Mei, M., Li, Z., Liu, S., & Wang, X. (2022). Study on Photocatalytic and Mechanical Properties of TiO_2 Modified Pervious Concrete. Case Studies in Construction Materials, 17, e01606. https://doi.org/10.1016/j.cscm.2022.e01606

[29] ASTM International (2017). ASTM C1701/C1701M-17a: Standard Test Method for Infiltration Rate of In-Place Pervious Concrete, West Conshohocken, PA, USA. https://www.astm.org/c1701_c1701m-17a.html

(This work is licensed under a Creative Commons Attribution 4.0 International License.)